Appl. Phys. B 54, 103–108 (1992)

Applied Physics B Photophysics and Laser Chemistry



# Quantitative CARS Spectroscopy of the $\nu_1$ Band of Water Vapour

**F. M. Porter and D. R. Williams**

Laser Spectroscopy Section, AEA Environment and Energy, Harwell Laboratory, Oxfordshire, OX11 0RA, UK

Received 1 October 1991/Accepted 11 November 1991

**Abstract.** The accuracy of CARS thermometry for $H_2O$ vapour has been assessed under carefully controlled conditions for the temperature range 295 to 900 K and the pressure range 0.0066 to 2.7 atm. Excellent agreement between theory and experiment was achieved for line-broadening regimes ranging from Doppler broadening to motional narrowing. Various models for rotational energy transfer and line-broadening were compared and where pressure broadening dominated, excellent agreement was achieved with a simple linewidth model, dependent only on temperature and pressure. Excellent agreement was also achieved using either energy or angular momentum based relaxation models to model motionally narrowed spectra in the pressure range up to 2.7 atm. However, good agreement between theory and experiment depended on the inclusion of state mixing correction factors, and good thermometry accuracy at high temperature was sensitive to the value assumed for the water molecular polarisability.

**PACS:** 42.65

Water vapour is of great importance as a heat transfer medium and as the only non-polluting combustion product. Coherent Anti-Stokes Raman scattering (CARS) has achieved considerable success in combustion thermometry [1], using $N_2$ as the probe molecule and $N_2$ thermometry accuracy is well established [2–5]. Data analysis for temperature measurement is generally carried out by comparing experimental data with a theoretical model and good thermometry accuracy depends on an accurate spectral model. This study aims to address the question of the accuracy achievable using water vapour CARS thermometry. The key to this is the accurate computation of water vapour spectra as a function of temperature and pressure. In a much earlier study [6], a comparison of theoretical and experimental spectra was presented for the pressure range 1 to 16 atm and 500 to 800 K. In that study we concluded that uncertainties in linewidth data limited the accuracy of calculated water vapour spectra. Information on self broadening Raman linewidths has recently been obtained by high resolution inverse Raman spectroscopy (IRS) measurements [7, 8]. In these studies Greenhalgh and Rahn found significant intensity discrepancies between theory and experiment for a small number of lines – these differences may arise from mixing between interacting vibrational states. Published CARS spectra also show differences between theory and experiment for particular, limited, spectral intervals [8]. The intensity correction factors determined in the IRS studies have therefore been included in the CARS model used here.

Spectral shape at high pressure is strongly influenced by motional narrowing effects – the accurate modelling of motional narrowing presents a major challenge for a molecule with the spectral complexity of water. Due to strong dipole–dipole interactions, water linewidths are considerably greater than those of, for example, nitrogen – motional narrowing effects have a marked effect on water vapour spectral shape even at ambient pressure.

It is possible to accurately model the molecular linewidths yet be unsuccessful in predicting motional narrowing. This can arise because motional narrowing depends on a smaller subset of state to state relaxation rates than do the overall linewidths. This has been observed for $N_2$, where models utilising an exponential energy dependence [4, 9] have proved most successful for pressures from 1–50 atm. By contrast, a simple polynomial energy gap [10] model is less successful in this regime and yet most accurately predicts motional narrowing at very high pressures [11]. An important part of the assessment of the thermometry accuracy has therefore been to study the ability of different models of rotational relaxation to model the motional narrowing process.

## 1 CARS Spectroscopy of Water Vapour

$H_2O$ is an asymmetric top molecule, characterised by three vibrational modes, a symmetric stretch ($\nu_1$), a bending mode ($\nu_2$), and an asymmetric stretch ($\nu_3$). All modes are Raman active but only $\nu_1$ is sufficiently intense to be of interest as a diagnostic; this has a Raman shift of 3657 $cm^{-1}$ and is strongly polarised. The Raman cross-section has been widely investigated [12–14], but the measured values cover quite a wide range. Several studies of the non-resonant background for water vapour have also been made [15, 16]. To accurately compute CARS spectra, very accurate energy level data is required and for this work a tabulation of energy levels comprising the published levels of Flaud et al. [17, 18] and unpublished data by R. Gaufres, kindly supplied by R.L.St. Peters, was used. The line intensities were calculated from the initial state thermal populations and the rotational and spin degeneracies. It was assumed that the vibrational Raman cross section did not vary between rotational states.

In their high resolution inverse Raman studies of the $\nu_1$ band of $H_2O$, Rahn and Greenhalgh [7, 8] compared the predicted intensity of transitions less than 98% $\nu_1$ in character with experimentally observed values. Significant discrepancies in intensity were noted for a number of lines and considerably improved agreement with the data was obtained by adjusting the line intensities or frequencies. Correlations between intensity corrections and fractional $\nu_1$ character were noted – these differences are likely to arise from mixing between interacting vibrational states. The differences were used to determine simple multiplicative factors for 21 states.

### *1.1 Linewidths*

At low pressure, linewidths arise from Doppler broadening. As gas density increases, the Doppler component of line broadening is reduced by Dicke narrowing, due to collisions which restrict the molecules' translational freedom. No Dicke narrowing was observed in the Raman study of Greenhalgh and Rahn [7, 8] although Grossmann and Browell's [19] study of water vapour in the infrared showed significant Dicke narrowing. Dicke narrowing can be expected to be more pronounced when the wavelength of the transition is of the order of, or larger than, the mean free path of the molecule and when the pressure broadening coefficient is small relative to the Doppler width – it may therefore be more important for the longer wavelength infrared transitions than for Raman.

As pressure increases, pressure broadening dominates the Raman linewidths. Considerable experimental and theoretical attention has been given to $H_2O$ linewidths and various theoretical approaches have been developed by Anderson, Tsao and Curnutte [20] (ATC), Davies and Oli [21] (QFT) and Robert and Bonamy [22, 23] (RB). More recently, Agg and Clary [24] have used the infinite order sudden (IOS) approximation to calculate rate constants for $H_2O$–$H_2O$ rotationally inelastic scattering. Recently [8], inverse Raman measurements were performed to obtain the first data on $H_2O$ broadening at above ambient temperatures.

To accurately model spectral shape at pressure, in addition to requiring accurate linewidths, a knowledge of rotational relaxation is needed so that motional narrowing effects can be calculated. Considerable success has been achieved in using so called fitting laws to model state to state relaxation rates by relating the rates to the energy difference between interacting states. In particular, laws utilising an exponential dependence on energy gap have accurately modelled $N_2$ [4, 9], CO [25] and $O_2$ [26]. More recently, Alwahabi et al. [27] have suggested an alternative approach, based on angular momentum rather than energy, which they have successfully applied to study $NH_2$ in collision with H atoms.

In general the collisional linewidth for the rotational state $J, \tau$ can be assumed to follow

$$\Gamma_{J\tau} = \Theta + \sum_{J'\tau' \neq J\tau} (\gamma_{J\tau J'\tau'}), \tag{1}$$

where $\Theta$ represents contributions from vibrationally inelastic and dephasing collisions, and $\gamma_{J\tau J'\tau'}$ represents the rotational relaxation rate from state $J'\tau'$ to $J\tau$. In their high resolution inverse Raman studies of $H_2O$ Greenhalgh and Rahn [7, 8] determined linewidths for a range of rotational states over the temperature range 300 to 1200 K. They obtained good agreement between these experimental results and both energy and angular momentum based fitting laws. For the former case, to obtain optimum agreement, they found it necessary to distinguish between relaxation for a given $J$ level and that between pairs of $J$ manifolds – this gave rise to a quantum differentiated energy gap law (QDEGL):

$$\gamma_{J\tau J'\tau'} = cPT^{-\alpha}\varrho_j(2J+1) \times \exp[(-\beta\Delta E_{\tau\tau'} - \beta\Delta E_{JJ'})/kT], \tag{2}$$

where $c$=26.6, $\alpha$=2/3, and $\beta$=1/3 and $\Theta$=0.2$P$300/$T$.

The relaxation rates using their collisional angular momentum exponent law (CAMEL) are:

$$\gamma_{J\tau J'\tau'} = cPT^{-1}\varrho_{J\tau}(2J+1)\exp[(-\beta|l|)/kT], \tag{3}$$

where the angular momentum $l$, transferred on collision is:

$$l^2 = -2(J^2+J-k_a^2-k_c^2)^{1/2}(J'^2+J'-k_a'^2-k_c'^2)^{1/2} + J^2+J+J'^2+J' - 2(k_ak_a'+k_ck_c'). \tag{4}$$

Optimum parameters were $c$=324.7 and $\beta$=47.0 $cm^{-1}$ for $\Theta$=0.1$P$300/$T$ and $c$=375.0 and $\beta$=34.0 $cm^{-1}$ for $\Theta$=0.0

The CARS spectrum frequency dependence can be expressed, following the treatment of Hall et al. [28], as

$$I(\omega) = sd \cdot G(\omega)^{-1} \cdot \tilde{P} \cdot d. \tag{5}$$

To calculate the motionally narrowed spectra requires the inversion of the $G$ matrix, which can typically involve over 200 states for a given parity at moderate temperatures. It is then necessary to calculate the convolutions over the pump linewidths to obtain the CARS signal [29].

## 2 Experimental

The CARS system used for these experiments is similar to that described elsewhere [4]. A frequency doubled, pulsed Nd:YAG laser provided 0.4 $cm^{-1}$ bandwidth pump beams and a broad-band dye laser with a corner cube retro-reflector to reduce the dye laser noise provided the Stokes beam. The

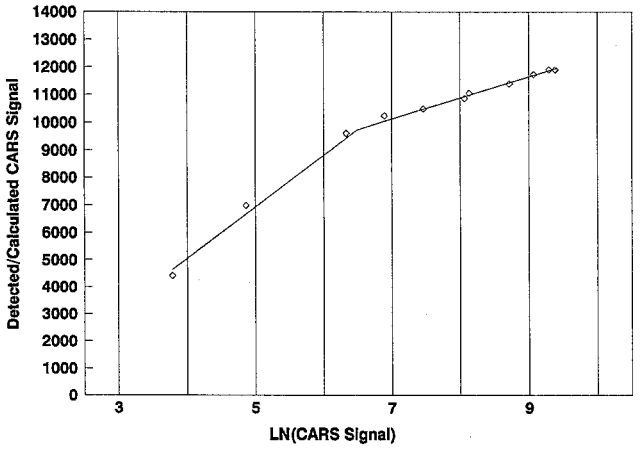


**Fig. 1.** Measured response of intensified photodiode array camera. The ratio of the diode array signal to a reference is plotted vs the natural logarithm of the diode array signal. In both cases the detector readout noise is first subtracted from the diode array signal (– calculated; ◇ averaged)

beams were combined using a folded BOXCARS geometry and the signal dispersed on a 1 m Czerny-Turner spectrograph fitted with a Tracor Northern Series 6133 intensified diode array camera. The dispersion of the signal was measured to be 0.00798 nm/diode at the water wavelength of 445 nm.

Nonlinearities in the response of the diode array camera used can distort the CARS spectrum shape and so reduce CARS thermometry accuracy. Because a different response can occur if the illuminating source is focused or not, a CARS signal was used to quantify any nonlinearities for the camera used. CARS signals from air in a temperature controlled laboratory were dispersed and detected on the camera. A series of carefully calibrated neutral density filters were used to attenuate the signal and a series of averaged and single shot CARS spectra measured. The unattenuated Nd:YAG laser strength was monitored before and after the experiment and no overall drift in signal levels observed. The response of the detector, as compared with that calculated on the basis of the neutral density filters, is shown in Fig. 1. This differs slightly from that observed in a previous study [4], where a diffused Nd:YAG laser provided the source. For the purposes of correcting measured spectra, the response was approximated by two logarithmic responses.

Water vapour was held at controlled conditions of temperature and pressure in a sealed quartz cell, similar to that of Rahn and Greenhalgh [7]. Briefly, the vapour pressure inside the cell was adjusted by controlling the temperature of the water in a sealed side arm which was kept as the lowest temperature in the system. The side arm was placed in a temperature controlled bath of water or ethylene glycol. A 50 cm long tubular observation furnace of 7 cm bore, comprising several concentric silica tubes, the innermost of which was heated, controlled the overall cell temperature. Shielded thermocouples monitored the temperature of the side arm, the link of the side arm to the main cell, and the outer wall of the cell. Measurements indicated that the temperatures within the cell walls agreed with those outside it to within 5 K. Prior to use the cell was heated with a flame to oxidise any residual hydrocarbon deposits.

For each measurement condition, four 50 s averaged spectra were measured, prior to background subtraction and rationing to a nonresonant background. At each condition the temperture of the side arm was first stabilised. A set of measurements were then made for different furnace temperatures, after the cell had reached equilibrium. Spectra were measured at 295, 425, 600, 745, and 900 K, at 0.0067, 0.02, 0.2, 0.37, 0.8, 2.0, and 2.7 atm. Within this range, safety limited measurements at 2.7 atm to low temperatures, signal strength limited measurements at 0.0067 atm to moderately low temperatures and the need to keep the side arm as the coolest part of the system limited measurements to low pressure at 295 K.

## 3 Results and Discussion

### *3.1 Low Pressure*

At low pressure, linewidths arise from Doppler broadening. Small inaccuracies in the pressure broadened linewidths are therefore minimised. A comparison between theory and experiment was made for low pressure data, ranging from 296 K and 0.0067 atm to 897 K and 0.017 atm. Under these conditions Doppler broadening accounted for between 80 and 92% of line broadening.

Separate comparisons were carried out with and without including the modifications to line intensity [8] discussed above. Generally excellent agreement was achieved. Including the modified intensities significantly improved the agreement between theory and experiment for all temperatures, particularly in the region of 3645 $cm^{-1}$. A comparison between modified and unmodified results is given in Fig. 2.

### *3.2 Pressure Broadening*

Prior to analysis of high pressure data, a comparison was made between spectra calculated using an averaged linewidth model [30], which was independent of line rotational state, and the QDEGL exponential gap model. The averaged model gave:

$$\Gamma = 27.911 P T^{-0.7622} . \quad (6)$$

Only very minor differences between calculated spectra were noted. The maximum variation in linewidth with rotational quantum number occurs at low temperatures, and so this represents the maximum discrepancy likely. As is shown in Fig. 3, the differences are slight. As observed by Hartmann [31] in his comparison of calculated water spectra, for moderate resolution measurements, averaged linewidth models give acceptable results. For the remainder of the low pressure calculations averaged linewidths were used.

Typical results of the data analysis are shown in Fig. 4. In general excellent agreement is obtained between theory and experiment. Temperature accuracies were generally within ±20–30 K, as is shown in Fig. 5. Because motional narrowing effects were neglected, higher inaccuracies were observed at 420 K at and above 0.8 atm. The agreement between theory and experiment at low temperature was very insensitive to the value of resonant to nonresonant suscepti-

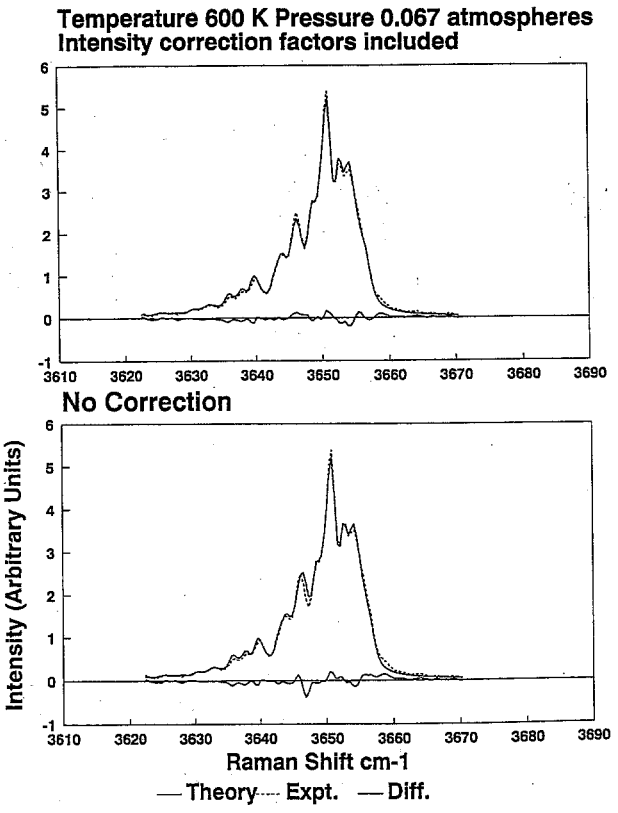


Fig. 2. A comparison of Doppler broadened water vapour spectra measured at 600 K and 0.0067 atm with and without modifications to line intensities

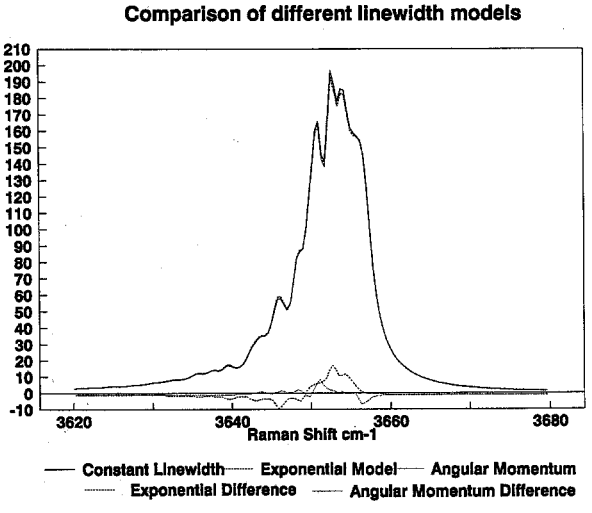


Fig. 3. A comparison of spectra calculated for 350 K and 0.25 atm, using an average linewidth, exponential energy gap, and angular momentum linewidth models. The difference between models has been expanded 5 times for clarity

bility used, because the resonant susceptibility is sufficiently strong to dominate the CARS signal. However, at high temperature and atmospheric pressure or above, the resonant contribution is reduced relative to the nonresonant background and the value of susceptibility used had a significant effect in particular on the quality of agreement and also on the thermometry accuracy. A reduction in the Raman cross section of 50% would result, at 900 K and one

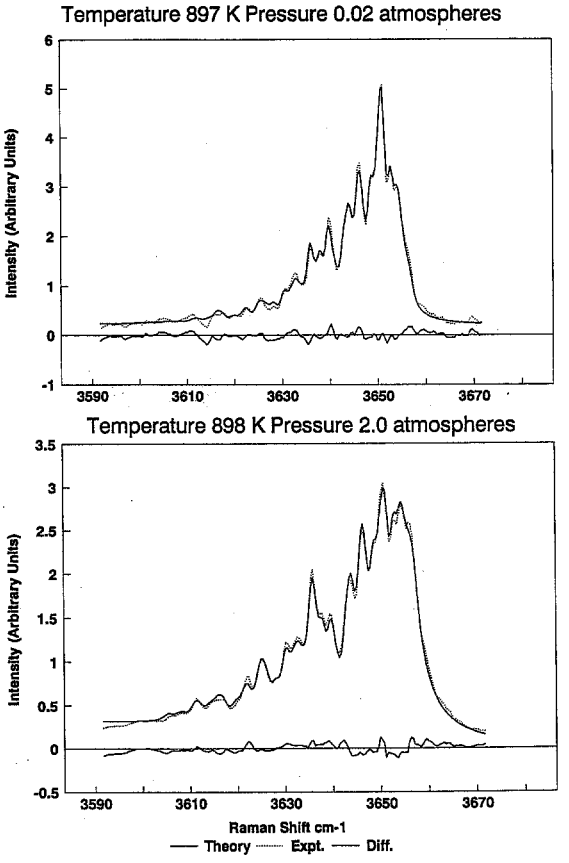


Fig. 4. A comparison of theoretical and experimental CARS spectra, at 897 K and 0.018 atm and 898 K and 2.0 atm

atmosphere, in temperature decreases of approximately 50 K, with a doubling of the residuals between theory and experiment. The nonresonant susceptibility of Farrow et al. [15], $1.85 \times 10^{-17}$ cm$^3$ erg$^{-1}$ atm$^{-1}$, was used. Measured values for the resonant susceptibility cover quite a wide range – optimum agreement with experimental data was obtained using a value of $1.24 \times 10^{-30}$ cm$^2$ sr$^{-1}$, slightly greater than that of Penney and Lapp of $1.1 \times 10^{-30}$ cm$^2$ sr$^{-1}$ [12], yet considerably less than that of $2.16 \times 10^{-30}$ cm$^2$ sr$^{-1}$ determined by Abe and Ito [13].

### 3.3 Motional Narrowing

A full $G$ matrix calculation was carried out for the Raman linewidths, using either the QDEGL or CAMEL models for rotational relaxation rates. This calculation included the computation of interstate relaxation for up to 240 states of either spin parity. To reduce computational times the efficient pre-diagonalisation method of Gordon and McGinnis [32], adapted for CARS by Koszykowski et al. [9] was used. The number of vibrational bands was reduced at low temperature. The full calculation of motional narrowing involving all these states was, however, very time consuming. Given that the line separation is such that all lines will not take part in the narrowing process, motional narrowing was calculated over a limited number of states, and the other lines

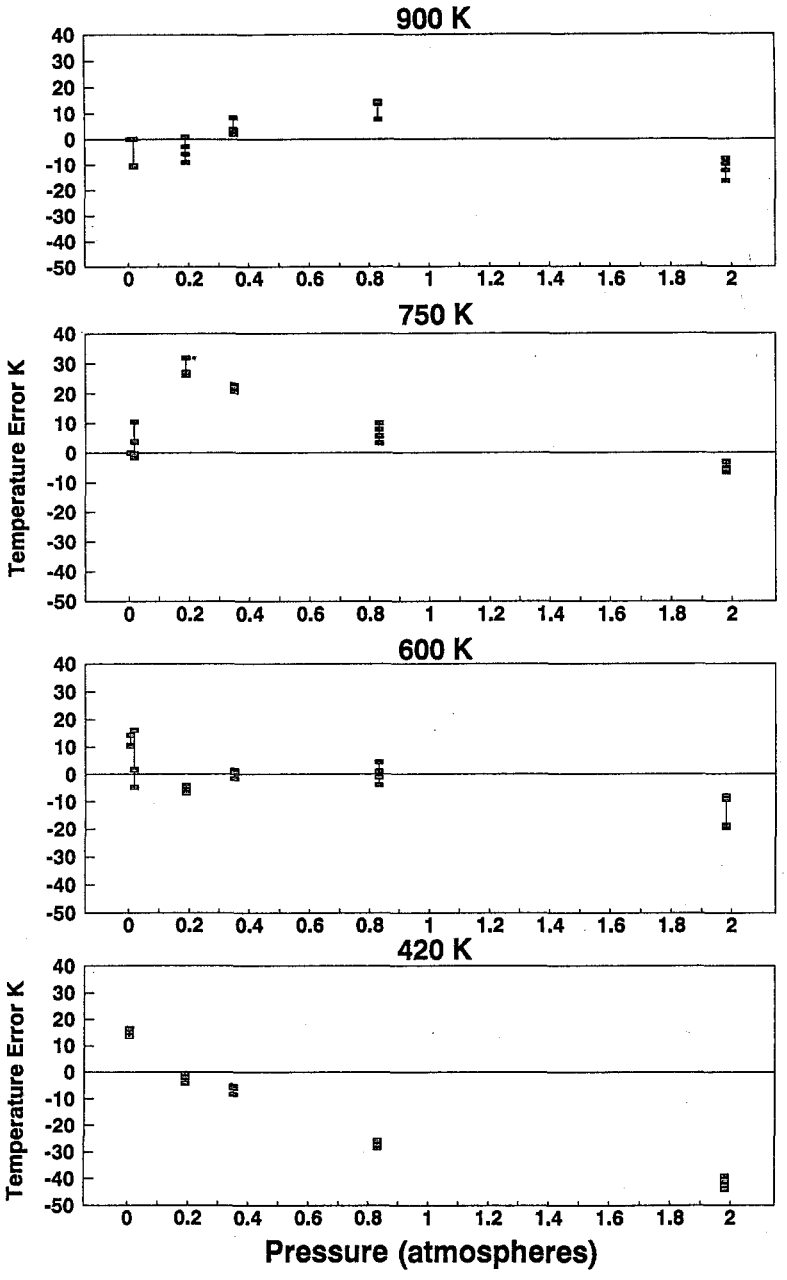


**Fig. 5.** Temperature measurement accuracy using the assumption of averaged linewidths and isolated lines

contributed to the spectrum shape in isolation. The number of states included was increased until no change in spectral shape was observed. Typically 20 states for each parity in the ground vibrational state were included at 400 K.

Excellent agreement was achieved using either angular momentum or energy gap models, with smaller differences between theory and experiment in the latter case. For the temperature and pressure range studied the differences between assumptions about the degree of vibrational relaxation present will also influence the accuracy of the models used. Typical results are shown in Fig. 6 for temperatures of 425 K at 2.7 atm. In these examples vibrational relaxation contributions of $0.2P300T\,\mathrm{cm}^{-1}$ were included for the exponential energy gap model (QDEGL) and $0.1P300/T\,\mathrm{cm}^{-1}$ for the angular momentum linewidth model (CAMEL). The corresponding temperature accuracies are given in Fig. 7.

In studies [4] of nitrogen CARS thermometry accuracy, it has been found that the nonlinear response of diode array detectors can make a significant contribution to CARS measurement errors. For the data in this study the CARS signals were automatically background subtracted and ratioed to a nonresonant background. Therefore the exact spectrum signal strengths were not retained and exact compensation for detector effects was not possible. However, peak signal heights were maintained closely in the region of 2500 counts and corrections were made on this basis – variations of ±300 counts have been found to have little effect. Correcting for nonlinearities in the detector response gave a small improvement in agreement between theory and experiment and an increase in fit temperature of approximately 10 K across the whole measurement range, a smaller effect than observed for nitrogen.

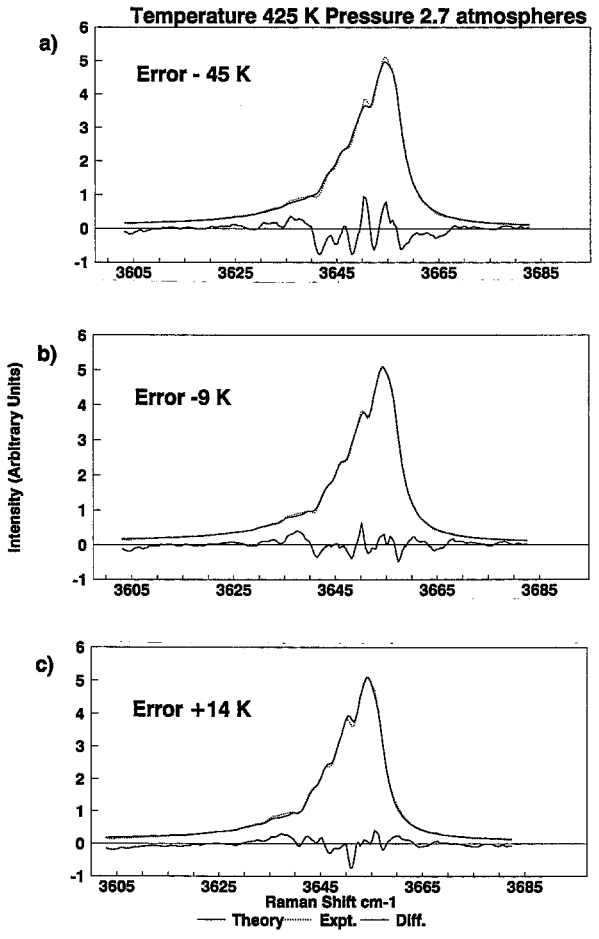


**Fig. 6a–c.** Experimental spectrum at 425 K and 2.7 atm compared to theoretical models, assuming **a** isolated lines, **b** exponential gap linewidth model (QDEGL), **c** angular momentum linewidth model. Vibrational relaxation has been included in the narrowing calculations. The difference between theory and experiment has been expanded 5 times for clarity

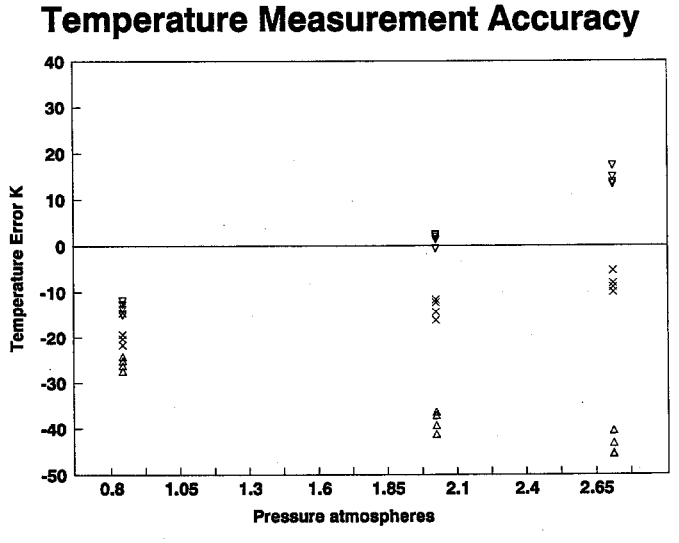


**Fig. 7.** Thermometry accuracy with the inclusion of motional narrowing effects (△ isolated lines; × exp. energy gap; ▽ angular momentum)

## 4 Conclusion

In conclusion, excellent agreement has been obtained between experimental CARS water vapour spectra and a theoretical model for pressures up to 2.7 atm. In this range both models based on energy and angular momentum transfer modelled motional narrowing effects well. Including the effect of the fractional $\nu_1$ nature of some transitions is required for optimum agreement. Temperature measurement accuracies within ±30 K were achieved for the range studied.

*Acknowledgements.* This work was supported by AEA Technology Underlying Programme. Special thanks are due to D.A. Greenhalgh (Cranfield Institute of Technology) and P.J. Agg and D.C. Clary (Cambridge University) for useful discussions and C.A. Baker (Epsilon Research) and S.J. Wood (Meteorological Office) for their assistance with the CARS measurements.

## References

1. D.A. Greenhalgh: In *Advances in Non-Linear Spectroscopy*, ed. by R.J.H. Clark, R.E. Hester, (Wiley, Chichester, UK 1988) pp. 193–251
2. M. Pealat, P. Bouchardy, M. Lefebvre, J.-P. Taran. Appl. Opt. **24**, 1012 (1985)
3. Th. Dreier, B. Lange, J. Wolfrum, M. Zahn: Appl. Phys. B **45**, 183 (1988)
4. F.M. Porter, D.A. Greenhalgh, P.J. Stopford, D.R. Williams, C.A. Baker: Appl. Phys. B **51**, 31 (1990)
5. M. Woyde, W. Stricker: Appl. Phys. B **50**, 519 (1990)
6. D.A. Greenhalgh, R.J. Hall, F.M. Porter, W.A. England: J. Raman Spectrosc. **15**, 71 (1984)
7. L.A. Rahn, D.A. Greenhalgh: J. Mol. Spectrosc. **119**, 11 (1986)
8. D.A. Greenhalgh, L.A. Rahn: J. Raman Spectrosc. **21**, 847 (1990)
9. M.L. Koszykowski, R.L. Farrow, R.E. Palmer: Opt. Lett. **10**, 478 (1985)
10. D.A. Greenhalgh, F.M. Porter, S.A. Barton: J. Quant. Spectrosc. Radiat. Transfer **34**, 95 (1985)
11. B. Lavorel: 10th European CARS Workshop, Dijon (1990)
12. C.M. Penney, M. Lapp: J. Opt. Soc. Am. **66**, 422 (1976)
13. N. Abe, M. Ito: J. Raman Spectrosc. **7**, 161 (1978)
14. I.I. Kondilenko, P.A. Korotkov, V.A. Klimenko, O.P. Demyanenko: Opt. Spektrosk. **43**, 645 (1977)
15. R.L. Farrow, R.P. Lucht, L.A. Rahn: J. Opt. Soc. Am. B **4**, 1241 (1987)
16. S. La, L.E. Harris: Appl. Opt. **25**, 4501 (1986)
17. J.M. Flaud, C. Camy-Peyret, J.P. Maillard: Mol. Phys. **32**, 499 (1976)
18. C. Camy-Peyret, J.M. Flaud: Mol. Phys. **32**, 523 (1976)
19. B.E. Grossmann, E.V. Browell: J. Mol. Spectrosc. **136**, 264 (1989)
20. P.W. Anderson: Phys. Rev. **76**, 647 (1949)
21. R.W. Davies: Phys. Rev. A **12**, 927 (1975)
22. B. Labani, J. Bonamy, D. Robert, J.M. Hartmann: J. Chem. Phys. **87**, 2781 (1987)
23. C. Delaye, J-M. Hartmann, J. Taine: Appl. Opt. **28**, 5080 (1989)
24. P.J. Agg, D.C. Clary: Submitted to J. Chem. Phys.
25. J.P. Looney, G.J. Rosasco, L.A. Rahn, W.S. Hurst, J.W. Hahn: Chem. Phys. Lett. **161**, 232 (1989)
26. G. Millot: 10th European CARS Workshop, Dijon (1990)
27. Z.T. Alwahabi, C.G. Harkin, A.J. McCaffery, B.J. Whitaker: J. Chem. Soc. Faraday Trans. 2, **85**, 1003 (1989)
28. R.J. Hall, J.F. Verdieck, A.C. Eckbreth: Optics Comm. **35**, 69 (1980)
29. D.A. Greenhalgh, R.J. Hall: Optics Comm. **57**, 125 (1986)
30. D.A. Greenhalgh, L.A. Rahn: Proc. 11th Int. Conf. on Raman Spectrosc. (Wiley, Chichester, UK 1988) pp. 143–144
31. J.M. Hartmann: J. Mol. Spectrosc. **127**, 35 (1988)
32. R.G. Gordon, R.P. McGinnis: J. Chem. Phys. **49**, 2455 (1968)